



Review

Critical discussion of the results from different corrosion studies of Mg and Mg alloys for biomaterial applications [☆]

Wolf-Dieter Mueller ^{a,*}, M. Lucia Nascimento ^b, Monica Fernández Lorenzo de Mele ^c

^a Dental and Biomaterial Research, "Charité" Universitätsmedizin Berlin, Assmannshauer Str. 4–6, 14197 Berlin, Germany

^b Technische Universität Berlin, Fachgebiet Werkstofftechnik, Str. des 17. Juni 135, Sekr. EB 13, 10623 Berlin, Germany

^c INIFTA and Universidad de La Plata, Facultad de Ingeniería, Diag. 113 y 64. CC 16 Suc. 4, La Plata, Argentina

ARTICLE INFO

Article history:

Received 31 March 2009

Received in revised form 30 October 2009

Accepted 29 December 2009

Available online 4 January 2010

Keywords:

Magnesium

Corrosion

Resorbable biomaterials

ABSTRACT

The aim of this work was to collect and compare data from different published reports which focused on the description of the influence of different electrochemical setups for the assessment of magnesium corrosion. Based on this, a comparison with our own results, obtained for LAE 442 and AZ 31, was made and discussed. As the collection of data has shown, the reported inconsistencies between in vivo and electrochemical data depend greatly on the electrochemical medium used, on the alloy composition and on surface preparation. Nevertheless, these differences also exist when comparing different in vitro results using different methodologies and even different Mg alloys, and need therefore to be discussed more thoroughly in the future. The simulation of transport conditions of the in vivo interface should become a focus of research interest in order to gain a better understanding of the influence of connecting processes on the degradation of the biomaterials.

© 2010 Acta Materialia Inc. Published by Elsevier Ltd. All rights reserved.

1. Introduction

During the last years, resorbable metallic materials have increasingly become a focus of interest of research, especially alloys of iron and magnesium [1].

Magnesium is an essential element which is a part of the bone structure. Dissolved Mg ions may promote bone cell attachment, tissue growth at the implants [2], and can be applied in surgical as well as in cardiovascular treatments [3,4].

The major concern over Mg alloys is their corrosion behaviour, and it is necessary to determine the corrosion rate and acquire knowledge of the corrosion mechanism in order to develop better adapted biomaterials for practical applications.

Mg and its alloys in aqueous solutions react and produce hydrogen according to Eq. (1):



In the presence of chloride ions the magnesium hydroxide dissolves by reacting into the soluble salt, MgCl₂ according to Eq. (2):



Atrens [5] and Song [6,7] have shown that the quantity of hydrogen can be measured and used for the interpretation of the results obtained from electrochemical measurements, and they have given an explanation of the negative difference effect (NDE), caused by the different amounts of hydrogen and Mg ions that do not fit with Faraday's law.

How and how fast these reactions take place depend on various parameters, such as:

- the composition of the Mg alloy;
- metallurgical treatments;
- the kind of surface treatment;
- the composition of the contacting electrolyte;
- the pH of the environment and buffer capacity of the electrolyte;
- the mechanical inputs such as compression or bending forces;
- the biological environment, presence of biological molecules, e.g., proteins;
- transport phenomena associated with the reactants and products of the corrosion reaction.

Some studies [4,8,9] have shown that the dissolution rate of implants in vivo is significantly reduced in comparison to results obtained under simulated in vitro conditions. However, the information taken from in vitro experiments allows the testing of newly developed alloys before these are placed in an animal.

Results obtained from electrochemical measurements seem to be in contrast to immersion tests results [10]. Nevertheless, they

[☆] Part of the Thermec'2009 Biodegradable Metals Special Issue, edited by Professor Diego Mantovani and Professor Frank Witte.

* Corresponding author. Tel.: +49 30 450562769; fax: +49 30 450562923.

E-mail address: wolf-dieter.mueller@charite.de (W.-D. Mueller).

give the possibility of obtaining information about the corrosion process much faster than the weight loss tests. Based on the corrosion current density and polarization resistance—obtained from the potentiodynamic curves—the corrosion activity, corrosion rate and the kind of corrosion process, such as uniform, pitting or filliform corrosion, can be predicted.

The corrosion resistance is directly related to the polarization resistance and inversely proportional to the current density measured at the equilibrium point. The shape of the curves gives an indication about the form of corrosion taking place at the surface, e.g., a constant current range indicates the formation of a passive layer; a symmetric logarithmic curve around the corrosion potential indicates clearly the situation of uniform corrosion; pitting or crevice corrosion can be assessed based on the shape of the anodic part of the i vs. E curve after the passive layer has been disrupted.

The main problem with the electrochemical assessment of corrosion phenomena is that in most cases more than one kind of corrosion mechanism has to be considered simultaneously. Therefore, complementary techniques should be used, especially based on microscopic views of investigated surface areas, to detect changes to the surface morphology.

In the case of the corrosion of Mg and Mg alloys the major problem for biomaterial application is not solely the hydrogen development: 0.01 ml cm^{-2} per day is a tolerated level in the human body according to Zeng et al. [11]. The major problem is the prediction of the evolution of corrosion rate, since that mechanical stability and degradation should be balanced so that as long as the healing process is going on, the mechanical stability by the biomaterial can be assured without its premature failure [12,13].

Another essential consideration with regard to corrosion is the influence of aggressive ions such as chloride ions, and large biomolecules such as peptides and proteins, on the corrosion rate and on the kind of corrosion process taking place, which might be the origin of the discrepancies between in vitro and in vivo responses.

In the past, various electrolyte compositions, especially with various Cl^- -ion level were used for corrosion analysis. The concentration of 3.5% NaCl [8] seems too different from the Cl^- -ion level in the body [13,14]. However, even concentrations lower than 0.9% NaCl can have an critical influence on the stability of Mg and Mg alloys [15]. Concerning the chemistry of magnesium, the fact that the reaction with phosphates, sulphates and carbonates can yield stable compounds, which can cover the surface and thus reduce the corrosion rate, ought not to be neglected. Xin et al. [2] demonstrated that, despite this layer formation, carbonates promote a uniform corrosion of Mg and that phosphates delay the emergence of pitting corrosion.

The average composition of blood plasma and of artificial body fluid (SBF), used by various authors is collected in Table 1.

The role of amino acids and proteins was also investigated in the past; instead of the expected reduction of corrosion and slight passivation behaviour, an acceleration of corrosion was observed, depending on the concentration of albumin [14,15,17–19].

The aim of this work was to collect and to compare the methodology and data from different published reports, which have focused on the description of the influence of different electrochemical setups for the assessment of magnesium corro-

sion. Based on this, a comparison with our own results was made and discussed.

2. Materials and methods

The electrochemical measurements for the comparison with citations were made using the Mini-cell-system setup (MCS). [20] This is a three-electrode system with a saturated calomel electrode (SCE) as reference electrode and a working electrode area of 0.8 mm^2 , which allows measurements at one and the same specimen by moving along its surface.

The wrought AZ31 and LAE 442 Mg alloys were tested, for a comparison with our own previously reported results [15,21]. The tests were performed in sodium chloride solutions of different concentrations, in PBS and in cell culture medium. The compositions of the electrolytes are collected in Table 2. Moreover, tests were performed on PBS containing different concentrations of bovine serum albumin (BSA).

The measurements were made at room temperature on polished surfaces.

3. Results and discussion

3.1. Comparison of literature results

Table 3 contains the data of various published investigations on corrosion of Mg and Mg alloy concerning biomaterial applications. This collection covered both the influence of material composition and the influence of the experimental setup.

The main point of interest is the comparability of the in vitro experiments with the in vivo observations. A second point of view is the comparability of the different in vitro experiments especially concerning the ranking of different parameters on the corrosion behaviour of Mg alloys.

The collection of the data demonstrates the variability of the results due to the different experimental conditions and shows the impossibility of comparing any of them in order to find reliable limits for prediction of the corrosion rate of Mg alloys. It seems that only the in vivo data should be relied on.

Even in this case there are some questions arising, looking at the data published by Witte [1] where, based on in vivo experiments, a corrosion rate of $1.205 \times 10^{-4} \text{ mm year}^{-1}$ for LAE 442 and $3.515 \times 10^{-4} \text{ mm year}^{-1}$ for AZ 91 were determined. According to Jones [29], such corrosion rates are outstanding from the point of view of corrosion resistance. In contrast, the corrosion rate analysed by electrochemical measurements are 6.9 mm year^{-1} for LAE and 2.8 mm year^{-1} for AZ91 performed in technical sea water. Despite this difference, the development and testing of new Mg alloys using reliable in vitro tests are necessary for the assessment of corrosion rates.

Considering the in vivo corrosion rate calculated by Witte et al. [1], it is impossible that a rod of a diameter of 1.5 mm and a length of 20 mm might be absorbed by the body during 18 weeks in a rat bone. Therefore, taking into account the volume loss over 18 weeks for AZ91 with 32 mm^3 and for LAE442 with 15 mm^3 over the whole

Table 1
Composition of blood plasma and SBF.

Concentration (mmol^{-1})	Na^+	K^+	Ca^{2+}	Mg^{2+}	Cl^-	HPO_4^{2-}	HCO_3^-	SO_4^{2-}	References
Blood plasma	142	5	2.5	1.5	103	1.0	27.0	0.5	[16,17,2,14]
SBF	142	5	2.5	1.5	103	1.0	10.0	0.5	[16,17,13]
	75 HEPES (and 0.6% albumin)								
SBF	109.5	6	7.5	1.5	110	3.0	17.5	0	[10]

Table 2

Composition of the electrolytes used in the tests.

	Cl ions (%)	Phosphates (%)	Carbonates (%)	Sulphates (%)	BSA (%)	Others 1	Others 2
NaCl	0.5–3.5	–	–	–	–	–	–
PBS	0.8	0.135	–	–	0–10%	–	–
Cell medium ^a	0.696	0.058 + HEPES	0.22	0.02	10	Vitamins	Amino acids: glucose

^a McCoy's 5A medium.

rod area (97.78 mm^2), the corrosion rate for both alloys *in vivo* is dramatically higher than reported: $0.95 \text{ mm year}^{-1}$ for AZ 91 and $0.44 \text{ mm year}^{-1}$ for LAE442.

Concerning the *in vitro* measurements, from the electrochemical point of view, a lot of parameters have to be considered, such as the Cl^- -ion concentration, the type and concentration of peptides, the buffer system and the type of measurement setup.

The hydrogen evolution reaction, a kind of “galvanic” reaction at the surface, is an important driving force for the corrosion reaction. It affects the Mg-ion concentration in the vicinity of the surface and it is also known to increase the pH of the interface, even in the case of buffered solutions.

This pH shift and the Mg-ion concentration influence the potential at the interface. However, these two factors cannot be resolved in the *in vitro* corrosion rate measurements. Therefore as long as the hydrogen development occurs and the surface of the Mg alloy is exposed to the electrolyte, electrochemical measurements will make sense. The question that remains is how close the calculated corrosion rate is with respect to the *in vivo* situation.

Concerning the measurement setup, with a reduction of the measurement area, the scan rate of assays can be increased and thus the measurement time is reduced, which gives the chance to exclude hydrogen during the measurements.

Based on this idea, measurements in different Cl^- -ions containing electrolytes with and without the addition of BSA were performed. The i vs. E curves obtained using the MCS setup are presented in Figs. 1 and 2; the corrosion current vs. the Cl^- -ion concentration, and vs. the BSA concentration, are shown in Figs. 3 and 4, respectively.

The following graphics show the data obtained for AZ31 and LAE442 using MCS setup. Fig. 1 shows the influence of surface treatment, comparing a ground surface (1200 SiC) and polished surface (6 μm with diamond paste). The measurements were performed in PBS containing different BSA amounts.

For the AZ31 alloy, the curves obtained for the polished surface are quite distinct from the ground surface curves. A clear passivation range and lower electrochemical activity can be observed for the polished surface. In comparison to this, the LAE alloy shows only little differences in both surface conditions. So it can be concluded that the corrosion rate of LAE442 depends less on the surface conditions than on the alloy AZ31.

Fig. 2 shows the influence of the electrolyte composition on the electrochemical response of AZ31 and LAE442 measured on the polished specimens.

It is interesting that for LAE442, the influence of the electrolyte composition is very small in comparison to AZ31. This is confirmed also by the electrochemical parameters, listed in Table 4.

The corrosion rate of AZ31 was strongly influenced by the electrolyte composition. In particular, for cell culture medium and Cl^- -free PBS, a relatively high corrosion rate was calculated. This is consistent with the remarks of Lim et al. [3], that the presence of a buffer changes the corrosion attack from localized or pitting to a more uniform corrosion process. Interestingly, analysing the corrosion rates in cell culture medium for AZ 31 and LAE 442 in detail, these results are also consistent with the *in vivo* results reported by Witte et al. [1].

Similar behaviour was reported by Rettig and Virtanen [17], concerning the corrosion rate of WE43 in SBF, which was significantly higher than in simple NaCl solution, showing that this alloy is also sensitive to the presence of buffer in the solution.

The data of the experiments published in Ref. [15] were newly assessed, focusing on the analysis of the influence of the Cl^- -ion concentration on the corrosion rate of Mg, AZ31 and LAE 442. Fig. 3 shows the dependence of i_{corr} as a direct parameter of the corrosion rate, vs. the Cl^- -ion concentration.

The dependence of i_{corr} on the Cl^- -ion concentration of the investigated materials showed that for Mg there was a dramatic decrease of i_{corr} with increase of Cl^- -ion concentration. LAE 442 shows a slightly linear increase of i_{corr} . For AZ31, i_{corr} decreases very slightly, except for 0.8% Cl^- -ion concentration.

This attests that it is not possible to compare the electrochemical measurements in electrolytes containing different amounts of NaCl, and based on it to make predictions about the corrosion behaviour of Mg-alloy-based devices. Such discrepancies are the reasons for misfits of electrochemical assessments in *in vivo* observations.

Fig. 4 shows the influence of added BSA in PBS. A completely different behaviour can be observed, in contrast to the influence of Cl^- ions as shown in Fig. 3.

Fig. 5 shows the influence of the amount of calcium in the alloy, on the corrosion current values in SBF electrolyte, compiled from Ref. [22]. From this, for low calcium contents (under 1 wt.% of alloy composition) a reduction of corrosion rate can be expected.

The influence of pH on the corrosion rate in electrolytes containing different amounts of chloride is presented in Fig. 6. This graphic depiction was made based on the data taken from Ref. [26]. The authors used different approaches and methodologies for the corrosion rate determination.

It is interesting to observe that between a pH of 7 and 11, the influence of the different factors is much lower than would be expected. Moreover, these differences are much smaller than at a pH of 3. An exception is the corrosion rate estimated by hydrogen development in higher NaCl concentration, at a pH of 7 and 11.

The open question that remains is the difference between this result and the one obtained by electrochemical measurements, because at a pH of 3 the results are comparable and relatively similar. The comparability of the methods is problematic, since it is theoretically not possible that the corrosion rate on steady state conditions (as were performed the hydrogen development measurements) is higher than for polarization measurements on a fresh prepared surface.

Concerning the albumin presence in PBS electrolyte, for LAE a higher corrosion rate was observed. This is in agreement with the albumin influence in SBF reported in Refs. [15,18,19] where at other alloys, an acceleration of corrosion in the presence of albumin could be observed. For the alloy AZ 31 the same result was observed for 1% albumin.

Returning to the comparison between *in vitro* and *in vivo* investigations as reported by Witte [1,8], the results might not be comparable because of the inadequate choice of electrolyte, seawater, rather than an inadequacy of the electrochemical methods for predicting *in vivo* behaviour of an Mg-based implant. Comparing our

Table 3

Collection of various published data concerning electrochemical characterization of pure Mg and Mg alloys.

Ref.	Alloys tested	Surface preparation	Degreasing agent	Area	Electrolyte	Electrolyte composition	OCP	CV	EIS	Amplitude	E_{corr} (V)	i_{corr} (μ A)	r_{corr} ($mm\ year^{-1}$)
[2]	AZ 91	4000 P	US ethanol	225 mm^2		NaCl; NaHCO ₃ ; K ₂ HPO ₄ ; Na ₂ SO ₄	OCP (SCE)	1 mV s ⁻¹	100 kHz 10 MHz	10 mV			
[10]	99.9% Mg	800 P	Acetone	280 mm^2	500 ml	SBF		Immersion test					3.0
[17]	WE 43	SiC/electropolishing in phosphoric acid	DMSO	490 mm^2	500 ml 37 °C	SBF SBF + albumin NaCl NaCl + CaCl ₂ NaCl + K ₂ HPO ₄	OCP 120 h (SSE)	1 mV s ⁻¹ Start: OCP –200 mV	100 kHz 10 MHz	10 mV			
[1,8]	AZ 91D LAE442		Isopropanol	113 mm^2		Seawater		Remark: immersion test, no reliable data					–0.3 5.5 2.8 6.9
		No data	Isopropanol	113 mm^2	RT	Borax-phosphate buffer pH 7	OCP SCE Start: –2 V 2 min	2 mV s ⁻¹	No	No			
	AZ 91D LAE 442							The electrochemical data is 3 times higher than the in vivo data for AZ91. In case of LAE442 is there is a factor of 23 ^a					0.9 0.3
[22]	AZ91 AZ91 + 1%Ca AZ61 + 0.4%Ca	2400 P	Aqua dest US ^c acetone	100 mm^2	37 °C	mSBF + HEPES pH 7.4	OCP 1 h SCE	0.5 mV s ⁻¹	100 kHz 10 MHz	10 mV	–1.73 –1.57 –1.71	65.7 17.8 36.5	1.1 0.3 0.6
													See Fig. 3
[21]	Mg AZ31 LAE442	1200 3 μ m diamond	Aqua dest	0.8 mm^2	RT 10 ml	NaCl various PBS PBS + BSA	OCP 5 min SCE	10 mV s ⁻¹ Start: –2.25 V	1 MHz 1 MHz	5 mV			See Figs. 1 and 2
[15]	Mg AZ31 LAE 442	1200 3 μ m diamond	Aqua dest acetone	0.8 mm^2	RT 10 ml	NaCl PBS PBS + BSA		10 mV Start: –2.0 V	No	No			
[23]	Mg–Mn Mg–Mn–Zn WE43	2000 P 0.5 μ m diamond	US ^c ethanol		350 ml 37 °C	SBF	OCP 20 min SCE	0.3 mV s ⁻¹ Start: –2 V	No	No	–1.85 –1.51 –1.70	57 79 16	0.7 0.54 0.48
[24]	AZ31 SC AZ31 ECAP AZ31 HR	4000 P			37 °C	Hanks sol		Immersion test					
[25]	Mg–Y–RE	4000 P 0.25 μ m diamond		100 mm^2		SBF (K9) Tris AP ^b	OCP SCE		100 kHz 10 MHz	10 mV			
[26]	ZE41	1200 P 0.5 μ m diamond	Aqua dest	100 mm^2	500 ml RT	0.1 + 1 M NaCl pH 3, 7, 11	OCP 48 h SCE	0.25 mV s ⁻¹					See Fig. 4
[27]	AZ 91D AZ 91anodized	1000 P		100 mm^2	200 ml	3.5% NaCl	OCP 20,000 s SCE	2.5 mV s ⁻¹	100 kHz 10 MHz	10 mV	–1.53 –1.38	38.4 0.18	0.09 0.3 17
[28]	Mg–1.2Mn–1.0Zn			$D = 1.5$ $L = 4$ mm		In vivo 18 weeks, loss: 55% Degradation rate in comparison with [21] 100 times smaller							0.55

^a 1. The in vivo data of Witte et al. [8] was calculated based on a loss of 30 mm^3 over 18 weeks, resulting in a corrosion rate of 0.9 $mm\ year^{-1}$.

$$CR = \frac{\Delta V}{\Delta t} = \frac{30\ mm^3}{98.7\ mm^2 \cdot 0.338\ year} = 0.9\ mm/year.$$

2. The corrosion analysis of in vitro tests was made using Tafel equations. According to this theory the scan rate used was too high. Usually the corrosion analysis should be performed after Mansfeld [29] over a range ± 20 mV around E_{corr} , which would produce lower corrosion rate values.^b AP, artificial plasma (6 times more carbonate than SBF).^c US, ultrasonic.

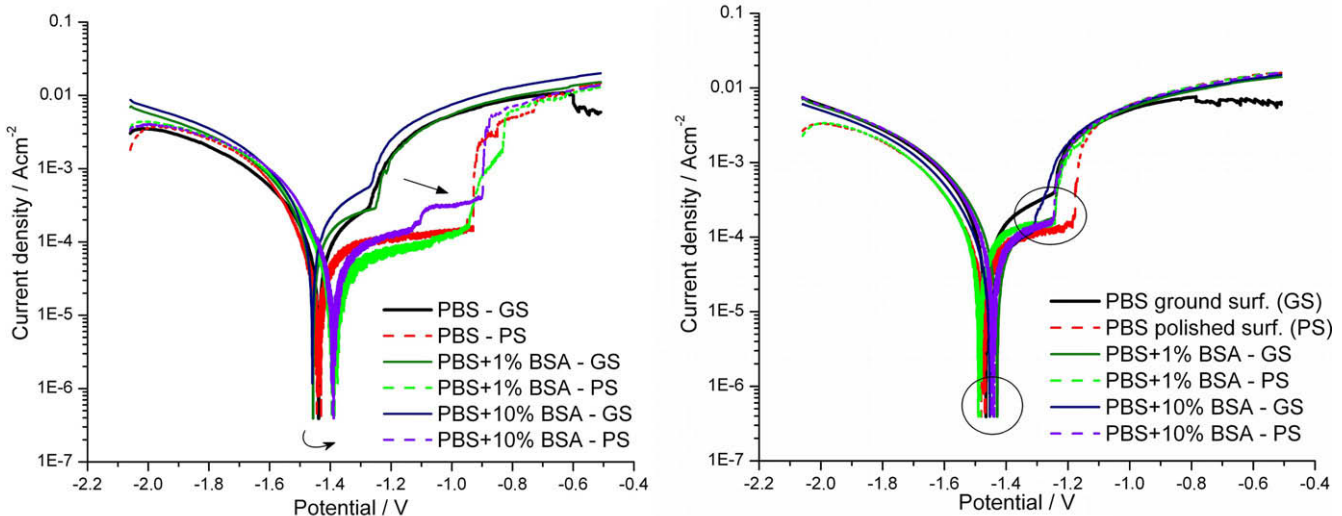


Fig. 1. Current density vs. potential (SHE) for AZ 31, on the left and LAE 442 on the right. GS, ground surface; PS, polished surface.

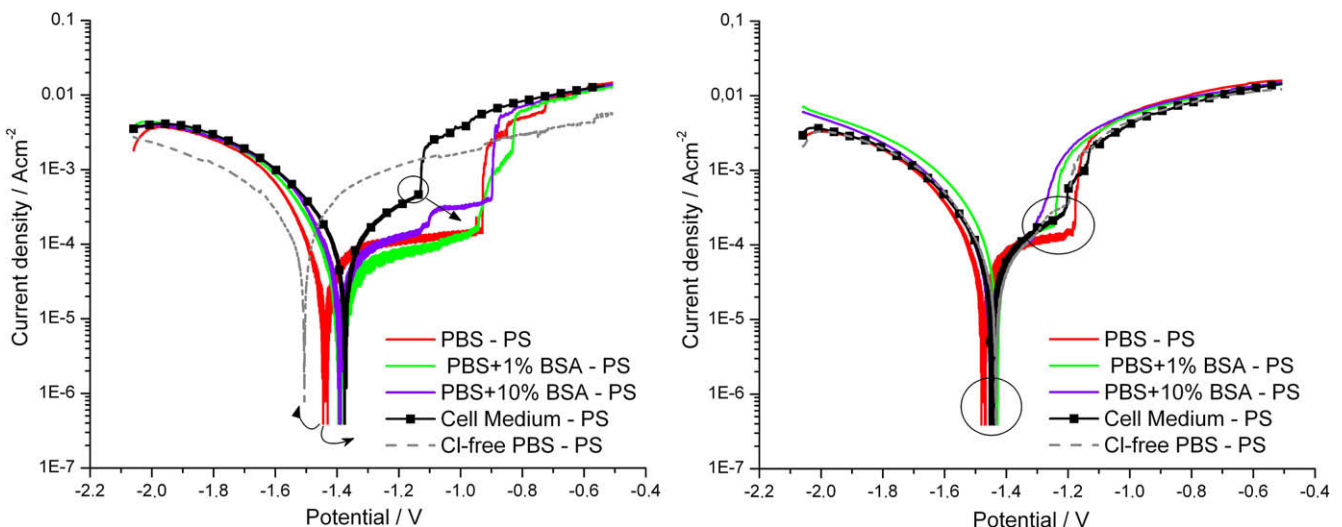


Fig. 2. Current density vs. potential (SHE) for AZ 31, on the left and LAE 442 on the right in different electrolytes. Arrows and circles indicate the changes in corrosion potential, corrosion current and breakdown potential.

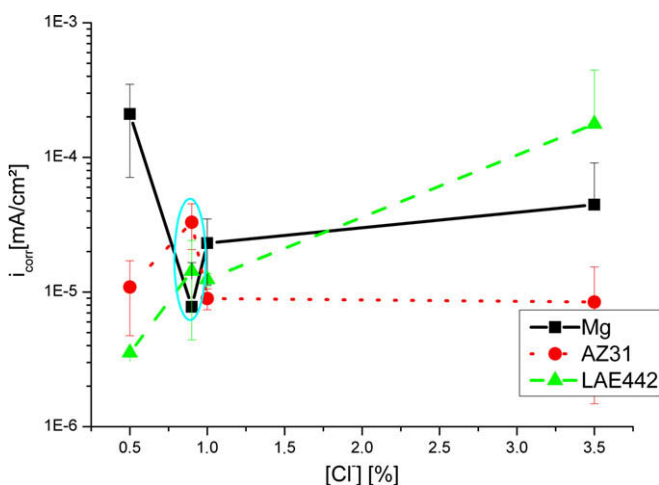


Fig. 3. i_{corr} vs. Cl-ion concentration for pure Mg, AZ31 and LAE 442 without any other added ions or peptides. Notice that the blue circle refers to PBS, a phosphate buffer containing 0.8% NaCl.

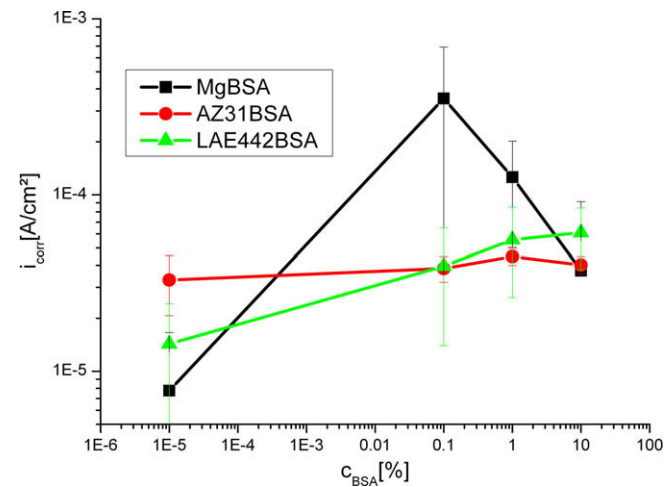


Fig. 4. i_{corr} vs. BSA concentration. Both axes are logarithmic scaled. Notice that the concentration of 10.5% of BSA is used for 0% BSA simply for a better presentation of this point on the logarithmic scale.

Table 4

Electrochemical data calculated from the current density–potential curves (Figs. 1 and 2).

	E_{corr} (V)	I_{corr} ($A\text{ cm}^{-2}$)	R_p ($\Omega\text{ cm}^2$)	E_{bd} (V)	r_{corr} (mm year^{-1})
AZ31					
Cell medium	−1.37	6.43×10^{-5}	404	−1.13	1.39
PBS	−1.44	2.65×10^{-5}	981	−0.93	0.57
PBS + 1%Alb	−1.39	3.43×10^{-5}	758	−0.94	0.74
PBS + 10%Alb	−1.39	2.60×10^{-5}	999	−0.9	0.56
Cl-free PBS	−1.51	9.75×10^{-5}	267	No passivation	2.11
LAE442					
Cell medium	−1.44	3.55×10^{-5}	733	−1.19	0.74
PBS	−1.47	3.49×10^{-5}	746	−1.18	0.73
PBS + 1%Alb	−1.49	4.96×10^{-5}	524	−1.24	1.04
PBS + 10%Alb	−1.44	5.75×10^{-5}	452	−1.25	1.20
Cl-free PBS	−1.51	3.57×10^{-5}	728	−1.2	0.73

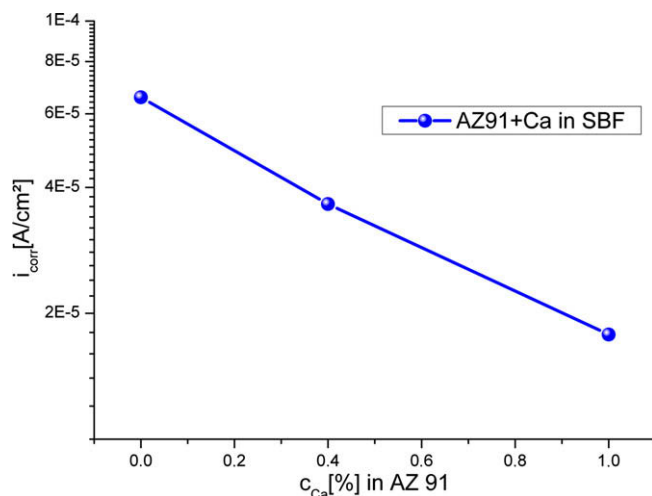


Fig. 5. Dependence of corrosion rate (i_{corr}) vs. Ca concentration in AZ91 according to Ref. [22].

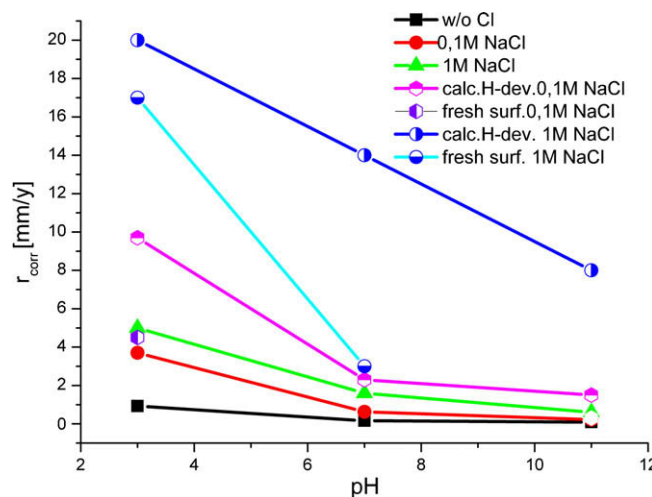


Fig. 6. Dependence of corrosion rate of ZE41 on the Cl-ion concentration; estimate based on different methods according to Ref. [26]. Calc, corrosion rate (r_{corr}) was calculated from hydrogen development measurements; fresh surf, r_{corr} was determined by electrochemical measurements on a freshly prepared surface; w/o Cl, without chloride.

results in cell culture medium (Table 4) with the in vivo results from Ref. [1] (in Table 3), it can be seen that the corrosion rate values for AZ31 was 1.5 times greater than in vivo AZ91, and for LAE it was 1.7 times greater. However, according to that, AZ31 would corrode two times faster when applied in the body, than LAE442. This is coherent with the observations made by Witte in vivo, where it was observed that the AZ91 implant was nearly completely dissolved after 18 weeks, whereas the LAE alloy was 70% intact.

Combination of measurement techniques such as electrochemical impedance spectroscopy (EIS), or even measurement techniques with microelectrodes as described by Lamaka [30], and the use of the SECM technique, as described by Amemiya for biological applications [31], could complement the CV data, in order to support the electrochemical in vitro results in comparison to in vivo experiments. This could help to reduce the use of animal tests in the initial stage of biomaterial testing.

4. Conclusion

As the collection of data has shown, the reported inconsistencies between in vivo and electrochemical data depend greatly on the used medium, on the alloy composition and on surface preparation. Nevertheless, these differences also exist when comparing different in vitro results using different methodologies and even different Mg alloys. In the future this should be the subject of further and thorough discussions.

The simulation of transport conditions of the in vivo interface should become a focus of research interest in order to gain a better understanding of the influence of connecting processes on the degradation of biomaterials.

Appendix. Figures with essential colour discrimination

Certain figures in this article, particularly Figs 1–6, are difficult to interpret in black and white. The full colour images can be found in the on-line version, at doi: 10.1016/j.actbio.2009.12.048.

References

- 1] Witte F et al. In vivo corrosion of four magnesium alloys and the associated bone response. *Biomaterials* 2005;26(17):3557–63.
- 2] Xin YC et al. Influence of aggressive ions on the degradation behavior of biomedical magnesium alloy in physiological environment. *Acta Biomater* 2008;4(6):2008–15.
- 3] Lim CS, Yong J, Toh KM. Manufacturing and near-physiological testing of a biodegradable metallic coronary stent (BMCS). *J Mech Med Biol* 2007;7(1):89–100.
- 4] Di Mario C et al. Drug-eluting bioabsorbable magnesium stent. *J Interv Cardiol* 2004;17(6):391–5.
- 5] Atrens A, Dietzel W. The negative difference effect and unipositive Mg⁺. *Adv Eng Mater* 2007;9(4):292–7.
- 6] Song GL, Atrens A. Understanding magnesium corrosion – a framework for improved alloy performance. *Adv Eng Mater* 2003;5(12):837–58.
- 7] Song GL, Atrens A. Corrosion mechanisms of magnesium alloys. *Adv Eng Mater* 1999;1(1):11–33.
- 8] Witte F et al. In vitro and in vivo corrosion measurements of magnesium alloys. *Biomaterials* 2006;27(7):1013–8.
- 9] Ren YB et al. Study of bio-corrosion of pure magnesium. *Acta Metall Sin* 2005;41(11):1228–32.
- 10] Wang Y et al. Corrosion process of pure magnesium in simulated body fluid. *Mater Lett* 2008;62(14):2185–8.
- 11] Zeng RC et al. Progress and challenge for magnesium alloys as biomaterials. *Adv Eng Mater* 2008;10(8):B3–B14.
- 12] Pietak A et al. Bone-like matrix formation on magnesium and magnesium alloys. *J Mater Sci Mater Med* 2008;19(1):407–15.
- 13] Witte F et al. Degradable biomaterials based on magnesium corrosion. *Curr Opin Solid State Mater Sci* 2008;12(5–6):63–72.
- 14] Yamamoto A, Hiromoto S. Effect of inorganic salts, amino acids and proteins on the degradation of pure magnesium in vitro. *Mater Sci Eng C Biomimetic Supramol Syst* 2009;29(5):1559–68.
- 15] Mueller WD et al. Degradation of magnesium and its alloys: dependence on the composition of the synthetic biological media. *J Biomed Mater Res* 2009;90A:487–95.

- [16] Virtanen S. Corrosion of biomedical implant materials. *Corros Rev* 2008;26(2–3):147–71.
- [17] Rettig R, Virtanen S. Time-dependent electrochemical characterization of the corrosion of a magnesium rare-earth alloy in simulated body fluids. *J Biomed Mater Res A* 2008;85A(1):167–75.
- [18] Liu CL et al. Degradation susceptibility of surgical magnesium alloy in artificial biological fluid containing albumin. *J Mater Res* 2007;22(7):1806–14.
- [19] Hao L, Lawrence J. The adsorption of human serum albumin (HSA) on CO₂ laser modified magnesia partially stabilised zirconia (MgO-PSZ). *Colloids Surf B Biointerfaces* 2004;34(2):87–94.
- [20] Mueller WD. Electrochemical characterization of metallic biomaterials with help of Mini Cell System (MCS). Habilitation, Humboldt-University of Berlin, 2009.
- [21] Mueller WD et al. Magnesium and its alloys as degradable biomaterials. Corrosion studies using potentiodynamic and EIS electrochemical techniques. *Mater Res* 2007;10:1–10.
- [22] Kannan MB, Raman RKS. In vitro degradation and mechanical integrity of calcium-containing magnesium alloys in modified-simulated body fluid. *Biomaterials* 2008;29(15):2306–14.
- [23] Xu LP et al. In vitro corrosion behaviour of Mg alloys in a phosphate buffered solution for bone implant application. *J Mater Sci Mater Med* 2008;19(3):1017–25.
- [24] Wang H, Estrin Y, Zuberova Z. Bio-corrosion of a magnesium alloy with different processing histories. *Mater Lett* 2008;62(15):2476–9.
- [25] Quach NC, Uggowitz PJ, Schmutz P. Corrosion behaviour of an Mg-Y-RE alloy used in biomedical applications studied by electrochemical techniques. *C R Chim* 2008;11(9):1043–54.
- [26] Zhao MC et al. Influence of pH and chloride ion concentration on the corrosion of Mg alloy ZE41. *Corros Sci* 2008;50(11):3168–78.
- [27] Zhang Y et al. Electrochemical behavior of anodized Mg alloy AZ91D in chloride containing aqueous solution. *Corros Sci* 2005;47:2816–961.
- [28] Xu LP et al. In vivo corrosion behavior of Mg–Mn–Zn alloy for bone implant application. *J Biomed Mater Res A* 2007;83A(3):703–11.
- [29] Jones DA. Principles and prevention of corrosion. 1st ed. New York: Macmillan; 1992. p. 568.
- [30] Lamaka SV et al. Monitoring local spatial distribution of Mg²⁺, pH and ionic currents. *Electrochim Commun* 2008;10(2):259–62.
- [31] Amemiya S et al. Biological applications of scanning electrochemical microscopy: chemical imaging of single living cells and beyond. *Anal Bioanal Chem* 2006;386(3):458–71.